NJC

Accepted Manuscript

This is an *Accepted Manuscript*, which has been through the Royal Society of Chemistry peer review process and has been accepted for publication.

Accepted Manuscripts are published online shortly after acceptance, before technical editing, formatting and proof reading. Using this free service, authors can make their results available to the community, in citable form, before we publish the edited article. We will replace this *Accepted Manuscript* with the edited and formatted *Advance Article* as soon as it is available.

You can find more information about *Accepted Manuscripts* in the Information for Authors.

Please note that technical editing may introduce minor changes to the text and/or graphics, which may alter content. The journal's standard Terms & Conditions and the Ethical guidelines still apply. In no event shall the Royal Society of Chemistry be held responsible for any errors or omissions in this *Accepted Manuscript* or any consequences arising from the use of any information it contains.

ROYAL SOCIETY OF CHEMISTRY

www.rsc.org/njc

New J. Chem.

PERSPECTIVE

Structured Catalysts for Dry Reforming of Methane

Mahesh Muraleedharan Nair[a] and Serge Kaliaguine*[b]

Received 00th January 20xx,
Accepted 00th January 20xx

DOI: 10.1039/x0xx00000x

www.rsc.org/

A major scientific challenge of the recent epoch is to develop practical processes that can convert greenhouse gases (CO_2, CH_4) into value added commodity chemicals or fuels. Dry (CO_2) reforming of methane (DRM) can be considered as an excellent option on this regard. DRM often requires a heterogeneous catalyst such as supported noble metals to efficiently convert CH_4 and CO_2 into synthesis gas (CO + H_2) which is extensively used in numerous industrial processes. Nickel based catalysts are considered as excellent low cost alternatives. However these catalysts undergo severe deactivation due to sintering of the active phase and/or coke (carbon) deposition on the surface. Significant control in the catalyst sintering along with enhanced coke resistance can be achieved if well defined structures (perovskites, spinels etc) are used as catalyst precursors or catalysts. Also, well controlled structured catalysts can be obtained by embedding the active phase into the pore channels of mesostructured materials (typically silica). This review is an attempt to summarize the recent progress in designing structured catalysts for the dry reforming of methane. Merits and demerits of these materials as provided by various authors will be discussed. It is believed that such a single platform will aid the scientific community to understand what is lacking for the fruitful development of sintering free, coke resistant catalysts to convert hydrocarbons into chemical feedstock by consuming two hazardous greenhouse gases.

Introduction

Being the major source of energy, fossil fuels presently have a huge impact on human welfare. The progressive depletion of their reserves coupled with the harmful effects of emission of greenhouse gases to the atmosphere put forward the need for alternate renewable and clean energy resources. For example, CO_2 being the main contributor of global warming, the emission of large quantities of this gas by the burning of fossil fuels demand immediate attention. On the other hand, CO_2 is the most abundant renewable carbon source and its chemical fixation into value added chemicals, is thus a highly promising strategy to counter the issues inherent with fossil fuels.[1] As to now, very few industrial processes utilize CO_2 as a raw material. The reason for this is that the carbon atom in CO_2 is in its most oxidized form and thus, a large energy input is necessary for the efficient transformation of this highly stable molecule.

Among other technologies,[2] dry reforming of methane (eqn.1) has received extensive attention from the global research community.[3]

$$CH_4 + CO_2 \longrightarrow 2CO + 2H_2 \quad \Delta H^0 = 247\ kJmol^{-1} \qquad (1)$$

This reaction involves the reforming of methane in presence of CO_2 over a heterogeneous catalyst to produce syngas (CO + H_2).

It is to be noted that this reaction also consumes methane which is the major component of natural gas and therefore abundant. The high purity syngas thus produced from DRM with H_2/CO = 1, serves the purpose of useful raw material for various industrial processes such as Fischer-Tropsch, for the production of various oxygenated chemicals or unsaturated hydrocarbons. Furthermore, due to its strong endothermicity, DRM can also be applied in energy transmission systems to convert inexpensive solar energy into chemical energy.[4] However; so far, no industrial practice has been established for DRM, mainly due to the absence of an effective catalyst. Therefore, developing efficient, stable and economical catalysts remains the bottle neck for commercializing this process.

The major concern that needs to be addressed is the development of catalysts with enhanced high temperature stability and activity. Regarding stability, severe carbon (coke) deposition on the catalyst surface during the course of the reaction is proven to be the main issue.[5] A number of studies devoted to the catalyst development were performed in the past among which noble metals occupy a prominent place. However these materials are costly and have limited availability.[3,6] Transition metal based catalysts, typically nickel and its derivatives, were developed as cost effective alternatives. In this case, investigation regarding the nature of supports, addition of promoters, catalyst preparation methods has been conducted, for enhancing the coke-resistance.[7] One method to improve the coke-resistance is to place the active phase (Ni) within a well-defined structure. Such structures could help to increase the temperature of the metal reduction closer to the reaction temperature. Reduction of the

[a] Department of Chemistry, Université Laval Quebec city, G1V 0A6, Canada.
[b] Department of Chemical Engineering, Université Laval Quebec city, G1V 0A6, Canada. E-mail: Serge.Kaliaguine@gch.ulaval.ca,Tel:+1 418 656 2708

crystalline oxide precursors (perovskites, spinels etc) that contain active metal species homogeneously dispersed inside the bulk leads to the migration of some of the metal atoms to the surface.[8] A highly dispersed active phase could be obtained in this way with increased coke-resistance. This method could also enhance the metal-support interaction and the thermal stability compared to that obtained by conventional impregnation methods. A more recent method to obtain confined Ni nanoparticles is to immobilize them inside the pore channels of ordered mesoporous silica materials such as SBA-15, SBA-16 or KIT-6[9] In this case, catalysts with extremely high values of specific surface areas can be obtained. Also, the large pore sizes (2-50 nm) and interconnected porosity of mesostructured materials are particularly helpful to overcome the mass transfer limitations suffered by their conventional counterparts.

This review is intended to convey a brief summary of the recent developments in designing structured catalysts for dry reforming of methane. The focus will be on mixed metal oxides with perovskite and spinel structures and mesoporous materials, in particular, silica incorporated with active metals and oxides. Regarding the mixed metal oxides, the presence of metal ions in the well defined structure was found to result in the formation of nanometer sized particles under reducing atmospheres. Also incorporation of multiple cations by partial substitution of the structure could result in a combination of elements which provides a promoting and/or stabilizing effect to the well dispersed catalyst particles obtained after reduction. In the case of mesoporous materials, the presence of pore channels yields high specific surface area and high dispersion of the active phase. Also, the confinement induced by the pore walls put forth a spatial restriction on the active phase, obstructing its sintering and thereby enhancing the stability under the conditions of operation.

Spinels

Spinels are mixed metal oxides represented by the general formula AB_2O_4, where A and B represent divalent and trivalent metal cations respectively. These interesting materials have been extensively studied as heterogeneous catalysts and as catalyst supports.[10] The presence of two catalytically active metal cations homogeneously dispersed in the structure makes them highly attractive. Recent studies clearly indicate that interesting results can be obtained for these materials owing to the synergy existing between the metal cations in the structure.[10]

In DRM, $MgAl_2O_4$ is an extensively studied spinel oxide, most commonly as a support. Guo *et al*. in 2004 compared γ-Al_2O_3, MgO-γ-Al_2O_3 and $MgAl_2O_4$ synthesized by co-precipitation as catalyst (Ni) supports.[11] The reactant feed ratio was CH_4/CO_2 = 1 with a flow rate of 30 ml/min. Their study indicated superior activity and stability for Ni/ $MgAl_2O_4$. In this case, approximately 90 % conversion was observed for both the reactants with a H_2/CO ratio closer to unity. Also, formation of an $MgAl_2O_4$ spinel layer in the case of Ni/MgO-γ-Al_2O_3 was observed which possibly suppressed the formation

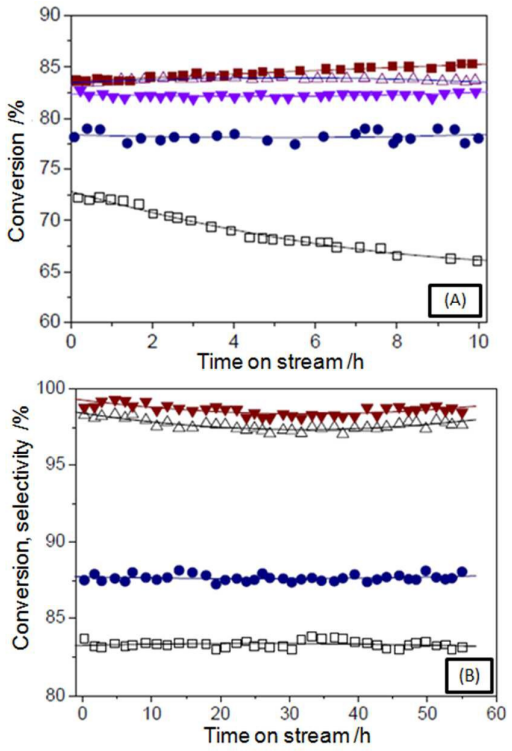

Fig. 1 (A) Dry reforming of methane at 750 °C over pre-reduced Ni/$MgAl_2O4$ catalysts with different Ni contents. (□) 1%, (●) 3%, (▼) 5%, (▲) 10% and (■) 15%. (B) Conversions of CH_4 (□), CO_2 (●), selectivity of CO (▼) and H_2 (Δ) at 750 °C over pre-reduced 5% Ni/$MgAl_2O_4$.[11]

of $NiAl_2O_4$ spinels and thus stabilized the tiny crystallites of Ni in this study. The authors attributed the observed high activity and coking resistance to the enhanced control over sintering, low acidity of $MgAl_2O_4$ and the interactions between Ni and $MgAl_2O_4$. In spite of a significant amount of carbon deposited, no deactivation was observed for 5 % Ni/$MgAl_2O_4$ catalyst for 55 h on stream at 750 °C (Fig. 1). Another study performed by these authors also indicated that the stability of Ni/γAl_2O_3 catalyst in DRM could be significantly improved by the addition of MgO.[12] In this case also, the enhanced stability was attributed to the formation of $MgAl_2O_4$ spinel layer which suppressed the possibilities for the formation of $NiAl_2O_4$. It is interesting to note that even though the formation of $NiAl_2O_4$ is generally considered to reduce the efficiency of the catalyst in DRM, improvement of coke resistance and hence enhanced stability is also attributed to the presence of this phase by some authors.[13]

Promotional effects of CeO_2 and ZrO_2 were found to further enhance the performance of $MgAl_2O_4$ supported Ni catalysts.[14] In particular, incorporation of low amounts of Zr in the CeO_2 structure provided dry reforming catalysts with enhanced stability. These highly dispersed, doubly promoted Ni catalysts with strong metal-support interaction showed significant suppression of formation of carbon. Recently Guczi *et al*. studied DRM with a feed composed of a mixture of 29 %

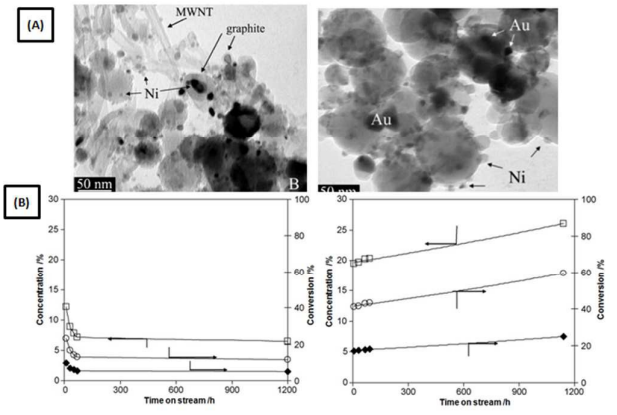

Fig. 2 (A) TEM images of $NiMgAl_2O_4$ and $NiAuMgAl_2O_4$ after the reaction with Ni grains, graphite crystals and nanotubes are visible in $NiMgAl_2O_4$. (B) CO concentration (□), and CO_2 (○) and CH_4 conversions (♦) at 675 °C on $Ni/MgAl_2O_4$ (left) and $NiAu/MgAl_2O_4$ (right).[15]

CO_2 and 71 % CH_4 over $Ni/MgAl_2O_4$ and $Au\text{-}Ni/MgAl_2O_4$ in a plug flow reactor.[15] In this study, the CO_2 conversion was found to be completed at 800 °C for both catalysts, with improved long term performance in the presence of gold. Concerning the role of surface carbon, it was reported that the $Ni/MgAl_2O_4$ catalyst was deactivated by graphite like carbon deposit and carbon nanotubes (CMWNT). On the catalyst containing Au, no graphite or CMWNT were observed, instead a carbonaceous species that can be easily gasified in presence of CO_2 was observed (Fig. 2). In this case, it was suggested that the amorphous NiC_x species formed in the first step on the catalyst surface further got transformed into graphite or CMWNT in the absence of Au. The addition of Au seemed to significantly retard this latter step.

Gonzalez-delaCruz *et al*. reported bimetallic catalysts with Ni/Co ratio 1:1 and 1:2 showing better activity and stability, with the XRD patterns indicating the formation of Ni-Co spinels.[10] An alloy formed by the reduction of these spinels contained adjacent nickel and cobalt sites that avoided the deactivation. The presence of Ni prevented the deposition of carbon over the cobalt sites and simultaneously the higher activity of the cobalt sites produced more hydrogen that helped to maintain the nickel atoms completely reduced under reaction conditions. This synergic effect accounts for the better performance of these bimetallic systems. deSouza et al. synthesized nanostructured Ni-containing spinel oxide catalysts.[16] For these materials, highly accessible Ni0 and/or Co0 sites were found to be responsible for the high catalytic performance in DRM. The NiCo (Co^0 and Ni^0 dispersed on $NiAl_2O_4$) and NiAl (Ni^0 dispersed on $NiAl_2O_4$) species were highly active for CH_4 conversion, whereas Ni^0 dispersed on either $Fe_3O_4\text{-}Co_3O_4$ or $CeO_2\text{-}NiAl_2O_4$ provided a lower catalytic performance due to active phase degradation. The higher activity exhibited by NiAl compared to NiCo was attributed to the higher activity of nickel for CO_2 decomposition, with stability due to the presence of well dispersed nanoparticles because they produced non-deactivating carbon deposits.

Benrabaa *et al*. compared the performance in DRM of $NiFe_2O_4$ prepared by co-precipitation, hydrothermal and sol-gel processes. The catalytic conversions were found to increase upon performing pre-reduction treatments. No coke formation was observed for these materials as evidenced by an oxidation step after the reaction. The authors attributed the observed catalytic behavior to the formation of nickel-iron alloy during the reduction process. The observed activity was higher for the materials made by hydrothermal and sol-gel processes. After a pre-reduction step at 400 °C, an improvement in conversions was observed for sol-gel prepared catalysts for which the conversions of CH_4 and CO_2 amounted to 80 and 93 % respectively at 800 °C, with $H_2/CO = 1.2$.[17] More recently, these authors observed that supporting $NiFe_2O_4$ on silica provides a more active and selective catalyst that seemed less prone to coking.[18]

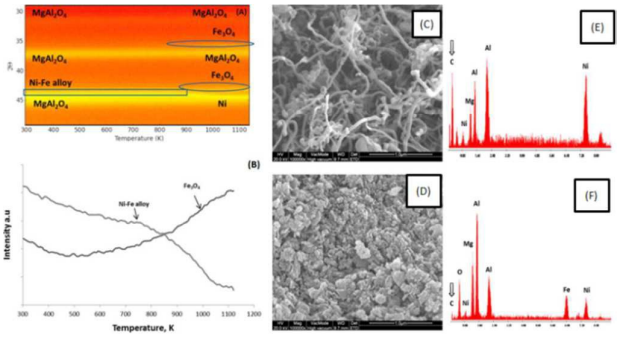

Fig. 3 In situ XRD during H_2-TPR: (A) 2D XRD pattern for 0.7-Fe/Ni, (B) integral intensity variation of (A) for diffraction areas 35.5–36.5° (NiO) and 43.7–44.2° (Fe-Ni alloy). SEM micrographs and EDX analysis of spent catalysts (temperature 1023 K, CH_4/CO_2 = 1/1, reaction time 4 h): (C) 0-Fe/Ni SEM image; (D) 1.1-Fe/Ni SEM image; (E) 0-Fe/Ni EDX; (F) 1.1-Fe/Ni EDX.[20]

Li *et al*. in 2015, reported novel nanocomposite structures for $Mg_x(Al)O$-supported NiCo bimetallic catalysts. These materials exhibited high coke resistance and long term stability for DRM. The catalytic performance was attributed to the synergy of diverse parameters such as particle size, catalyst size and alloying effect.[19] Theofanidis *et al*. in the same year examined a series of bimetallic $Fe\text{-}Ni/MgAl_2O_4$ catalysts with Fe/Ni ratios up to 1.5 for DRM under atmospheric pressure at 650–800 °C.[20] During H_2-TPR up to 700 °C, Fe_2O_3 and NiO were reduced to Fe and Ni. Higher temperatures lead to Fe-Ni alloy formation. The alloy remains stable up to 623 °C under CO_2-TPO and then decomposed to Ni and Fe_3O_4 at further higher temperatures. The Fe-Ni alloy is the active phase while Fe partially segregates from the alloy forming FeOx during dry reforming. This is beneficial as the surface carbon accumulation is reduced through interaction with FeOx lattice oxygen, producing CO. Alternate CH_4 and CO_2 pulse experiments over Ni, Fe, and Ni-Fe samples showed that dry reforming over Fe-Ni catalysts can follow a Mars–van Krevelen mechanism. A molar Fe/Ni ratio of 0.7 provides the most active and least deactivated catalyst (Fig. 3). All studied catalysts can be regenerated by CO_2 carbon removal. Kathiraser *et al*. synthesized Ni supported $LaAlO_3\text{–}Al_2O_3$ (NLA) perovskite and carried out DRM. The formation of $LaAlO_3$

perovskite involved interaction with octahedral sites of the alumina support, resulting in an enhanced Ni–Al interaction when Ni was impregnated. As a result, the inverse $NiAl_2O_4$ spinel structure was formed, which significantly affected the activity with the lowest carbon deposition. Enhanced stability of the NLA catalyst for 30 h at 800 °C was attributed to the enhanced lattice stability imparted by the inverse spinel structure and $LaAlO_3$.[21]

Perovskites

Perovskites are mixed metal oxides with general formula ABO_3, for which A and B represents two metal cations. In these materials, both A and B site ions can be partially substituted by other metals to form multi cation substituted perovskites ($AA'BB'O_3$). Among this category, the most common ones used for the dry reforming reaction are those having Ni in the B site of the structure. Such materials can be used as the precursors to obtain highly dispersed Ni catalysts by the direct reduction of the perovskites. Almost all the previous studies employed rare earth and transition metals respectively as the A and B site cations.[22] While the B site metal serves as the active site, the A site metal imparts stability and enhances the catalytic performance.

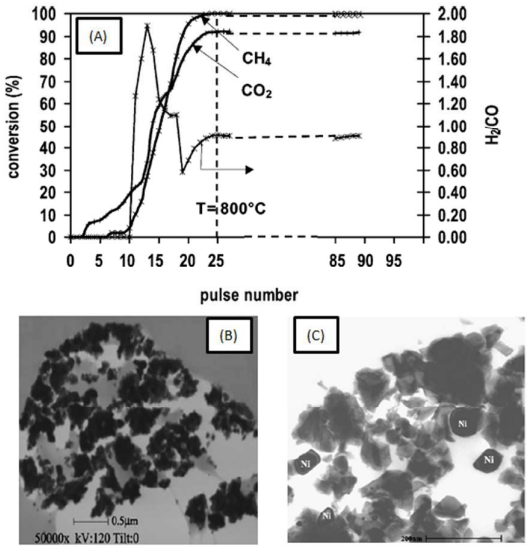

Fig. 4 (A) CH_4, CO_2 conversion, H_2/CO ratio versus the number of pulses and reaction temperature: 800 °C. (B) STEM image of $LaNiO_3$ calcined at 700 °C before the reaction. (C) STEM image of $LaNiO_3$ after reaction at 700 °C.[22]

Initial reports regarding the use of perovskites for dry reforming of methane came in 2003.[22] Batiot-Dupeyrat *et al*. used $LaNiO_3$ as catalyst precursor for the CO_2 reforming of methane. The reaction was studied by a pulse technique using a CH_4/CO_2 ratio close to unity. By performing a pre-reduction step, $LaNiO_3$ was transformed into La_2O_3 and Ni^0. 100 % conversion of CH_4 and 92 % conversion of CO_2 were observed at 800 °C with a H_2/CO ratio equal to 0.91 (Fig. 4). A mechanism involving the partial re-oxidation of La_2O_3 and Ni^0 by CO_2 followed by reduction back to La_2O_3 and Ni^0 by CH_4 was proposed by these authors to explain the presence of the observed crystallographic phases and the formation of syngas. Following this, Goldwasser *et al*. studied $Ln_{1-x}Ca_xRu_{0.8}Ni_{0.2}O_3$ (Ln = La, Sm, Nd) perovskites synthesized by a modified citrate method.[22] These perovskites were first reduced at 700 °C, to obtain nominal compositions of (Ru,Ni)/CaO and/or La_2O_3, Sm_2O_3, Nd_2O_3, before the catalytic tests. The authors observed Sm containing perovskites to be the best among the lanthanide series. The efficiency and stability were attributed to the formation of very small Ru–Ni nanoparticles (<20 nm) during the reduction step. $La_{0.8}Ca_{0.2}Ru_{0.8}Ni_{0.2}O_3$ and $La_{0.5}Ca_{0.5}Ru_{0.8}Ni_{0.2}O_3$ showed the highest selectivity to CO among the series. A strong influence of the A-site cations was observed on the stability and selectivity. In particular, Ca substitution was found to decrease the stability and lowered the reduction temperature of perovskites. The best overall performance was observed in the case of $LaRu_{0.8}Ni_{0.2}O_3$ with conversions of 89 % and 72 % for CH_4 and CO_2 respectively, and CO selectivity close to 90 % after 150 h on stream.[23] In the case of Sr substituted $LaNiO_3$ perovskites synthesized by the auto combustion method, it was observed that catalytic activity depends on Sr content ($LaNiO_3$ > $La_{0.6}Sr_{0.4}NiO_3$ > Ni (5 %)/La_2O_3 > $La_{0.9}Sr_{0.1}NiO_3$). The $SrCO_3$ and $La_2O_2CO_3$ phases formed during the reaction were proposed to be responsible for the lack of carbon deposition. These studies were performed using the pulse technique.[8]

Later, Batiot-Dupeyrat *et al*. reported high activity and stability for the CO_2 reforming of methane for the $LaNiO_3$ perovskite prepared by the auto-ignition method.[24] Here, the authors observed in situ reduction of the perovskite precursor during temperature increase up to 700 °C in the presence of the reactants (CH_4 and CO_2). Smaller Ni^0 particles were found to be produced in this way in comparison to the pre-reduction of $LaNiO_3$. CH_4 and CO_2 conversions up to 90 % were obtained with a H_2/CO molar ratio equal to 1 for more than 100 h. The high activity was attributed to the high dispersion of the Ni^0 particles which resulted from the in situ reduction. Partial substitution of Ni by Fe in $LaNi_{1-x}Fe_xO_3$ (x=0, 0.2, 0.4 and 0.7) resulted in a significant decrease in the conversion rates of both reactants with however a slightly enhanced stability of the catalyst.[25] On the other hand, in the case of Co substitution on $LaNiO_3$ perovskites, CH_4 and CO_2 conversions near 100%, was observed except for $LaCoO_3$ that showed a poor activity. These studies were performed between 600 - 800 °C under a continuous flow of the reactants. The as-synthesized solids were reduced during catalytic tests to form Ni^0, Co^0 and $La_2O_2CO_3$ which are responsible for the high activity and inhibition of carbon formation. The authors attributed the high activity to the in situ formation of Ni^0-Co^0 particles highly dispersed on $La_2O_2CO_3$ matrix that inhibited coke formation. Dopant Co stabilized Ni^0 particles suppressing coke formation, while the presence of small quantities of Ni was found to favour the reduction of Co and hence to accelerate the activation of the solid.[26] Rivas *et al*. synthesized a series of $LaNiO_3$ perovskites by the citrate method and by co-precipitation using K_2CO_3 as precipitating agent.[27] Crystalline

oxides were obtained with particle size variations depending on the method of synthesis. Co-precipitation produced the smallest Ni particles that seem to sinter during the reaction. On the other hand, the citrate method produced metal crystallites that exhibited better thermal stability. Their results also indicated the influence of the synthesis procedure on the performance of these solids by forming different lanthanum phases during reaction. It was observed that the partial substitution of nickel by rhodium (5% mol) yielded an increase in catalytic activity. No deactivation was observed for all these catalysts after 24 h on stream. In a similar study Johansson *et al*. synthesized $LaRhO_3$ by following a modified Pechini method. H_2 TPR indicated that the reduction of Rh in the perovskite structure occurred in two steps. CO and H2 formation was found to occur at 400 °C and 100 % conversion of both the reactant gases were observed at 600 °C. Side reactions such as RWGS and Boudouard reaction were also observed in this study. Interestingly when a pretreated (H_2 TPR at 950 °C) catalyst was used, it was observed that the reaction didn't start until 570 °C. However in this case side reactions were not observed. The authors suggested that H_2 TPR at 950 °C resulted in the formation of a single type of catalytically active sites for DRM which do not catalyze the side reactions.[28]

Gallego *et al*. studied the kinetic behaviour of the Ni/La_2O_3 catalyst obtained from the $LaNiO_3$ perovskite during DRM as a function of temperature and CH_4 and CO_2 partial pressures.[29] Considerable resistance to carbon deposition was observed under the reaction conditions. The model thus developed seemed to fit very well the experimental data, and the rate expression predicts better the rate of methane conversion than the models which incorporate only metallic clusters as the active sites. The apparent activation energies were lower than that reported for noble metal catalysts. Ni particles after the reaction were partially covered by $La_2O_2CO_3$ formed by interaction between La_2O_3 with CO_2. Catalytic activity occurs at the Ni-$La_2O_2CO_3$ interface, while the oxycarbonate species participate directly by reacting with deposited carbon, thus restoring the activity of the Ni sites at the interface. Gallego *et al*.[30] also compared the activity and stability of Ni catalysts, obtained from the reduction of $LaNiO_3$, $LaNi_{1-x}Mg_xO_{3-\delta}$ and $LaNi_{1-x}Co_xO_{3-\delta}$ catalysts, for CO_2 reforming of methane. During the reduction using H_2 at elevated temperatures, the perovskites are destroyed partially or completely and Ni nanoparticles are generated as catalysts. They found that the catalysts obtained from $LaNiO_3$ and $LaNi_{1-x}Mg_xO_{3-\delta}$ show better activities, compared with those containing cobalt. The increasing amount of Mg leads to a decrease in the coke formation. Later on, Gallego *et al*. studied the effect of Pr and Ce substitution on the A site of $LaNiO_3$.[31] After reduction, the average diameter of Ni^0 obtained from $LaNiO_3$, $La_{0.9}Ce_{0.1}NiO_3$ and $La_{0.9}Pr_{0.1}NiO_{3-\delta}$ were 15 nm, 9 nm and 6 nm respectively. The highest catalytic activity was obtained with the catalyst which was produced from the $La_{0.9}Pr_{0.1}NiO_{3-\delta}$. CH_4 and CO_2 conversions and the H_2/CO molar ratio were 49 %, 55 % and 0.81, respectively with no detectible carbon deposits after 100 h of reaction. The high resistance to deactivation was attributed to the lower Ni^0 particle size as well as to the redox chemistry of Pr_2O_3. In another study regarding the deactivation of $LaNiO_3$ in presence of H_2S, it was observed that the deactivation becomes faster by increasing the H_2S concentration.[32] Nickel sulfides with different stoichiometry (Ni_xS_y), lanthanum oxysulfide (La_2O_2S) and lanthanum sulfide (LaS_y) were observed.

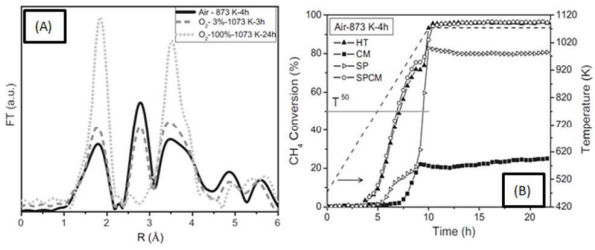

$LaNiO_3$ reduced (20mg)	H_2/CO	T_{CH4}^{50} (K)
▲ Hydrothermal	1.00	903
■ Combustion	0.63	-
▷ Spray pyrolysis	0.87	1040
○ Spray pyrolysis+Combustion	0.99	885

Fig. 5 (A) Fourier Transforms of the Ni K-edge EXAFS spectra obtained for the LaNiO3-CM after treatments: (a) air 873 K, 4 h; (b) O2 (3%)–He 1073 K, 3 h and (c) O2 (100%) 1073 K, 24 h. (B) CH_4 conversion, H_2/CO at 1073 K (t = 12 h) and temperature at 50% of CH_4 conversion (T^{50}_{CH4}) for $LaNiO_3$ catalysts.[31]

Pereniguez *et al*. studied catalytic properties of a Ni/La_2O_3 catalyst obtained by reduction of $LaNiO_3$ synthesized by various methods.[33] Although not evidenced by XRD data, XAS and TPR measurements show the presence of an amorphous NiO phase together with the crystalline $LaNiO_3$ phase (Fig. 5). The catalyst showed good stability under dry reforming of methane reaction conditions. This performance has been explained by the high resistance of the nickel particles to oxidation, as detected by in situ XAS. The effect of the presence of the amorphous NiO phase was reported by the same authors in 2012.[34] The larger amount of the NiO phase induces the formation of big Ni^0 particles after its reduction that reduces the catalytic activity. Pavlova *et al*. synthesized $LnFeNi(Ru)O_3$ perovskites using modified Pecchini method. The structural and redox properties and the catalytic performance were found to depend upon Ln nature and Ru content in the structure. Under reaction conditions, perovskites got converted to Ni–Fe(Ru) alloy particles and LnO_x epitaxially bound with Ln–Fe–O perovskites. A synergetic effect between Ni and Ru is reflected in the enhanced stability of perovskites to reduction as well as in a higher catalytic activity and resistance to carbon deposition for more than 20 hours in dry reforming of real natural gas. The resistance to coking of these catalysts in dry reforming of real natural gas containing admixtures of higher hydrocarbons is explained by combined effects of Ni dilution by Ru in alloy nanoparticles and the high mobility and reactivity of surface/lattice oxygen in the disordered Ln ferrite support.[35] Bhavani *et al*. synthesized Ba substituted $LaMnO_3$ ($La_{1-x}Ba_xMnO_3$ (x = 0.10–0.50) and used as catalysts for DRM.[36] The optimally substituted perovskite (Ba = 0.10 and 0.15) catalysts showed improved reducibility of Mn^{3+}/Mn^{4+} to Mn^{2+} which resulted in the donation of lattice

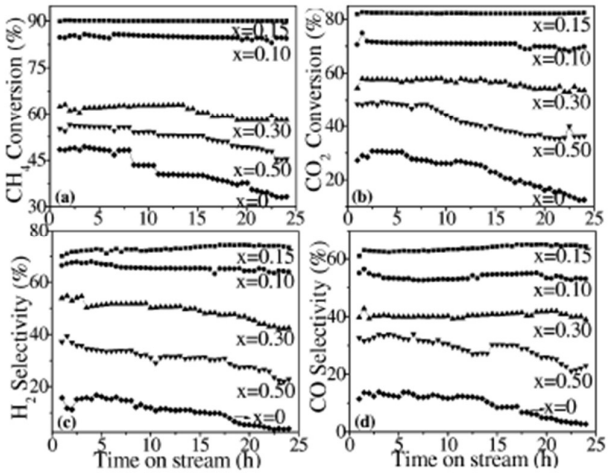

Fig. 6 Catalytic activity for dry reforming of methane with CO_2 over $La_{1-x}Ba_xMnO_3$ perovskite oxide catalysts: (a) CH_4 conversion, (b) CO_2 conversion, (c) H_2 selectivity, and (d) CO selectivity.[36]

oxygen towards the catalytic cycle. High conversions, syngas selectivity and stability with little coke formation was observed for these materials (Fig. 6). Odedairo *et al*. developed a template free approach for the synthesis of $LaCr_{0.9}Ni_{0.1}O_{3-\delta}$ nanowires. These nanowires exhibited higher CO_2 conversions compared to their bulk counterparts which were attributed to the enhanced exposure of active sites. The unique flower-like morphological structure of these materials resulted in enhanced dispersion of supported Pd nano particles resulting in an excellent performance and stability in DRM, and therefore in a higher turnover frequency for CH_4 (6.04 s^{-1}). The Pd decorated $LaCr_{0.9}Ni_{0.1}O_{3-\delta}$ exhibited remarkable long-term stability with no significant loss in conversion at 750 °C for 12 h.[37] Su *et al*. studied the performance of Ce substituted $LaNiO_3$ for DRM. The catalysts were synthesized using the Pechini method. 94 % and 92 % conversions were observed for CH_4 and CO_2 respectively at 800 °C for unsubstituted $LaNiO_3$.[38]

Mesostructured Materials

Ordered Mesoporous Silica

Ordered, silica mesostructures are intrinsically preferred catalyst supports due to their high specific surface area, large pore size, interconnected porosity and tunable heteroatom compositions. In addition, the confined space inside the pore channels will aid well controlled formation of nanoparticles of the catalytically active material. Grafting or embedding an active species onto mesoporous silica surfaces has opened new pathways for catalyst design.[39] Recent studies demonstrated a substantial beneficial effects of mesoporous materials in the CO_2 reforming.[40]

As early as in 1998, Wang and Lu studied the effects of the support phase (Al_2O_3, SiO_2 and MgO) and catalyst preparation methods on the activity and stability for the reforming reaction of methane with carbon dioxide.[41] This study indicated that the pore structure of the support and metal-support interaction significantly affected the catalytic activity and coking resistance. Catalyst with well-developed porosity exhibited higher catalytic activity. Strong interaction between metal and support made the catalyst more resistant to sintering and coking, thus resulting in a longer time of catalyst stability. González *et al*. synthesized a series of supported Ni-Co catalysts by impregnation of a mesoporous silica material (INT-MM1).[42] Catalytic activities were compared with a $LaCo_{0.4}Ni_{0.6}O_3$ perovskites synthesized by the citrate method. Significant differences in activity and product distribution were observed among the catalytic systems in the reforming reaction. The supported materials were active for the reaction, but selectivity for H_2 depended on the bimetallic composition of each solid. The different product distributions observed was attributed to the properties of the support and metal-support interaction. The selectivity towards H_2, reached 78 % in the case of supported catalysts. The perovskite derived catalyst was however the most active, with conversions up to 91 %. Both catalyst systems were quite stable up to 100 h on stream. Zhang *et al*. investigated a novel type of catalyst comprising Ni nanoparticles embedded in a mesoporous titania/silica support (Ni/TS) prepared using a combined impregnation/sol–gel method[40] The Ni/TS catalyst had a high BET surface area, small NiO particle size, high mesoporosity and high activity and stability (30 h) for DRM. Even though carbon nanotubes and encapsulated carbon were found on the surface, Ni/TS materials exhibited high activity and stability, which were attributed to the participation of carbon species as a reaction intermediate in the DRM reaction.

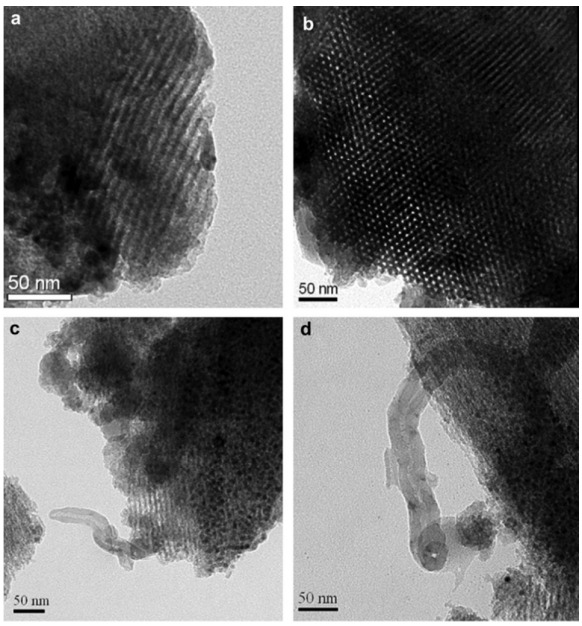

Fig. 7 TEM images of Ni/Ce-SBA-15: (a) fresh Ni/Ce-SBA-15; (b) spent Ni/Ce-SBA-15; (c), (d) filamentous carbon over spent Ni/Ce-SBA-15.[46]

Damyanova *et al*. synthesized a series of mesoporous MCM-41 with different Ni content (Ni/Si ratio of 0.2–0.4).[43] The effect of Pd addition on the catalytic properties for DRM of these materials was studied. These studies indicated that the

addition of a small amount of Pd (0.5 %) to Ni-containing catalysts lead to formation of small nanosized, easy reducible NiO particles. Formation of filamentous carbon over surface of spent monometallic Ni and bimetallic Pd-Ni catalyst were observed. However the activity and stability of bimetallic Pd-Ni catalysts were higher than those of monometallic Ni containing ones. Within bimetallic system, the Pd-Ni catalyst with Ni/Si ratio of 0.3 revealed the best performance and stability. In a similar study by Arbag *et al*. Rh was used as the promoting agent for Ni-substituted mesoporous MCM-41 catalysts by using both impregnation and hydrothermal synthesis techniques.[44] They observed that although the same amount of Rh was used to promote the catalyst, the catalyst synthesized by impregnation showed deactivation after 11 h of DRM at 600 °C. However, the hydrothermally synthesized Rh promoted catalyst had enhanced activity and long term stability. The hydrothermally synthesized Rh bimetallic catalysts showed lower selectivity for RWGS as compared to impregnated bimetallic catalysts. Thus these authors suggested that the synthesis method has a significant effect on the stability of the catalyst. Similarly, Ni incorporated MCM-41 synthesized by the hydrothermal method were studied for DRM by Yasyerli et al.[45] In this case, Ni/MCM-41 (Ni/Si molar ratio of 0.2), containing different amounts of Ru (0.5 - 3.0 wt%) and Mg (1 and 5 wt%) were synthesized using sequential impregnation of Ru and Mg into Ni/MCM-41. Dry reforming of methane was studied in a tubular flow reactor in the temperature range of 500 - 600 °C with different CH_4/CO_2 ratios in the feed stream. Quite high hydrogen yield values and improved stability of these catalysts indicated the promoting effects of Ru for the Ni/MCM-41 type catalysts. Ru incorporation (1.0% Ru) was shown to improve H_2 yields. Mg impregnation into Ru@Ni/MCM-41 improved catalytic performance by increasing CH_4 conversion and decreasing the contribution of reverse water gas shift reaction, especially at initial times (first 60 min). Coke formation by decomposition of CH_4 contributed to the hydrogen selectivity, but did not cause significant change in catalytic performance, especially at longer reaction times.

Wang *et al*. synthesized a series of Ce-incorporated SBA-15 mesoporous materials which were further impregnated with 12 wt.% Ni. The Ce/Si molar ratio had a significant influence on the catalytic performance on DRM. The highest catalytic activity and long-term stability were obtained over the Ni/Ce-SBA-15 (Ce/Si = 0.04). The improved catalytic behaviour was attributed to the cerium impact in the framework of SBA-15, where cerium promoted the dispersion of nano-sized Ni species and inhibited the carbon formation. In comparison with the effect of CeO_2 crystallites in SBA-15, cerium in the framework of SBA-15 promoted the formation of the nickel metallic particles with smaller size. The mesostructural order was kept intact after reaction and the pore walls of SBA-15 prevented nickel aggregation (Fig. 7).[46] Zhang *et al*. prepared Ni-ceria nanoparticles (Ni/Ce = 1/1) inside the cage-like pores of ordered mesoporous SBA-16 and used them as catalysts in DRM.[47] The confinement effect of the mesopores and the interaction between Ni and CeO_2 resulted in the formation of uniformly sized Ni nano particles (5.7 nm). Ceria addition facilitated the reduction of NiCe/SBA-16. Stable conversions were observed for up to 100 h at 700 °C (Fig. 8). The performance was attributed to the influence of CeO_2 and mesoporous framework on the structural stability of Ni particles. Kaydouh *et al*. carried out DRM over mesoporous SBA-15 containing 5 wt % Ni and 6 wt % Ce.[48] The mesostructural order and metal dispersion inside the pores were found to be preserved after metal addition and calcination. The most active catalyst was the Ni–Ce/SBA-15 sample prepared by impregnating cerium first, then nickel inside SBA-15. 100 % CH_4 conversion was obtained below 650 °C. Impregnation of Ce after Ni resulted in clogging of the pores and a lower activity than the impregnation performed in the other order. Xie *et al*. synthesized Ce modified mesoporous silica impregnated with Ni nanoparticles by a sublimation-deposition strategy.[49] Homogeneous distribution of Ni nanoparticles (2.1 to 4.3 nm) was obtained by this method. Carbon deposition was found to be negligible with near equilibrium conversion for CH4 and CO2 for 20 h was observed for this catalyst. The coke resistance of these catalysts were attributed to the presence of Ce. Liu *et al*. synthesized Ni containing ordered mesoporous KIT-6, by a one-pot co-assembly method, in which Ni species were highly dispersed into the pore walls. Compared with the catalyst prepared by conventional impregnation method, Ni-KIT-6 demonstrated extremely smaller Ni particles on the support and stronger interaction of Ni with the silica matrix. As a result, it exhibited a high catalytic activity and selectivity, and more importantly, good coke-resistant performance for the catalytic reaction of methane reforming with carbon dioxide.[50]

Xie *et al*. synthesized high dispersed Ni nanoparticles inside SBA-15 using a polyol route.[51] Polyol (ethylene glycol, glycerol or ethanol) coordinated Ni^{2+} was impregnated inside the pore channels of SBA-15. Intermediate carbon template resulting from the decomposition of polyol, prevented the migration of Ni particles from the pore channels. Removal of the carbon template under air followed by the reduction treatment resulted in the formation of highly dispersed Ni nanoparticles. In DRM, the conversion of CO_2 was found to be higher than CH_4. The performances of the catalysts prepared using ethylene glycol and glycerol were found to be better than the ones prepared using ethanol. Further Ni-SBA15 synthesized using ethylene glycol was found to exhibit higher long term stability (20 h at 750 °C) which was attributed to the enhanced sintering resistance and coking resistance. The confinement effect of pore walls prevented the sintering of Ni particles and thus enhanced the coking resistance.

Guo *et al*. studied the effect of reaction temperature, catalyst composition and support using a series of Ni based catalysts with KIT-6 and SBA-15 as supports.[52] CH_4 and CO_2 conversions over La_2NiO_4/KIT-6 reached 100 % when the reaction temperature was increased to 800 °C with GHSV of 3.36 x 10^4 mL $g^{-1}h^{-1}$ and CO_2/CH_4 molar ratio 1.1:1. Among La_2NiO_4/KIT-6, $LaNiO_x$/KIT-6 and $LaNi_2O_x$/KIT-6 catalysts, La_2NiO_4/KIT-6 presented the highest activity and stability. This

was possibly due to the fact that after reduction of the catalysts, La_2O_3

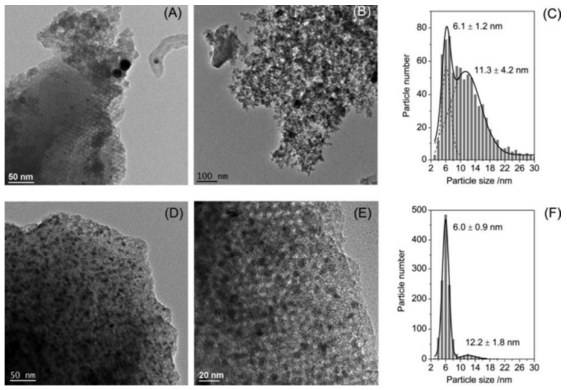

Fig. 8 TEM images of (A, B) used Ni/SBA-16 and (D, E) used NiCe/SBA-16 after catalytic reactions at 700 °C for 100 h, with Ni particle size distributions for (C) used Ni/SBA-16 and (F) used NiCe/SBA-16 catalysts.[47]

acted as a barrier and suppressed the aggregation of Ni particles during the reaction. With the increasing amount of La_2O_3 promoter, Ni particles were homogeneously distributed. Meanwhile, when compared with La_2NiO_4/SBA-15, stability test showed that the deactivation rate of La_2NiO_4/SBA-15 was faster than that of La_2NiO_4/KIT-6. This corresponded to the unique cubic structure of KIT-6, which was favourable for the diffusion of the reactant and product molecules during the reaction. Du *et al*. used mesoporous SiO_2 coated modular Ni-MgO-Al_2O_3 nano-platelets as catalysts for DRM.[53] These materials were synthesized by depositing organosilicate shells over layered double hydroxide (LDH) platelets. Subsequent calcinations and reduction resulted in the formation of Ni-MgO-Al_2O_3 nano-platelets with mesoporous silica shells. These materials displayed better performance in comparison with the conventional impregnated catalysts. The better performance of these modular catalysts with enhanced coke and sintering resistance were attributed to the dual confinement effects of the mixed oxide nano-platelets and the mesoporous silica shell.

Other Mesoporous Materials

Sun *et al*. synthesized Ni–CaO–ZrO_2 catalysts with different pore structures to be used as catalysts for DRM.[54] The catalyst with a mesoporous framework with a specific surface area of 210 m^2g^{-1} showed both high activity and stability. In particular, no deactivation was observed over a period on stream (100 h, 700 °C, GHSV = 12000 $mlg^{-1}h^{-1}$). The enhanced efficiency and resistance to coking was attributed to the confinement effect of the mesoporous structure which prevented Ni particles from sintering. Peters *et al*. in 2011 prepared highly porous and thermally stable ZrO_2 with high specific surface area up to 156 m^2g^{-1}, and with a tunable mesopores in the range of 3–10 nm by a template-assisted route using dodecylamine (DDA) and a post treatment in NH3 solution at different pH.[55] The high specific surface area was attributed to the incorporation of silicon (2.5 wt %) which was dissolved from glass vessels used during the post-treatment of the zirconia hydrogel at high pH values. 5% Ni-ZrO_2 showed good activity and selectivity in the dry reforming reaction. Methane conversions up to 75 % with hydrogen selectivities up to 87 % were obtained, which are clearly higher than those of zirconia supported catalysts prepared by conventional precipitation. In another study by Xu *et al*. ordered mesoporous NiO–Al_2O_3 composite oxides with different nickel content were synthesized via an improved evaporation induced self-assembly (EISA) strategy with Pluronic P123 as template. It was observed that these mesostructured catalysts exhibited high catalytic activity and long stability, with approximately 90 % conversion at 800 °C. The improved catalytic performance was suggested to be closely associated with both the amount of accessible active centers for the reactants on the mesopore wall surface and the stabilization of the active sites by the alumina matrix due to the confinement effect induced by the mesopores. The ‘‘confinement effect’’ in the mesoporous structure of the materials contributed in preventing Ni particles from sintering under severe reduction and reaction conditions. The stabilized Ni nanoparticles had strong resistance to carbon deposition, accounting for no deactivation after a 100 h long-term stability test at 700 °C.[56]

Shen *et al*. synthesized ordered mesoropous Ni–Al and Ni–Mg–Al oxides by evaporation induced self-assembly (EISA) using Pluronic P123 as a soft template. These ordered mesoporous catalysts exhibited much higher activity and durability for DRM. The specific surface area and ordered pore structure were found to be preserved for 30 h at 750 °C. The sintering of Ni was prevented and the coke formation was suppressed on these materials. The addition of Mg was found to enhance the coke resistance of these materials.[57] Newnham *et al*. prepared Ni-incorporated mesoporous alumina (MAl) materials with different Ni loading (7, 10 and 15 wt %) by a template assisted hydrothermal method for DRM.[58] The most active catalyst tested (10 wt% Ni)-MAl) displayed stability over 200 h compared to conventional materials of same composition, which had a significant loss in activity after 4 h of testing. The high stability of the Ni-MAl materials was attributed to the sintering resistance of Ni nanoparticles under the reaction conditions used (800 °C at a space velocity of 52,000 $mLh^{-1}g^{-1}$). The low susceptibility of the Ni nanoparticles in these catalysts to migration/sintering was most likely due to a strong Ni - support interaction and/or active metal particles being confined to the mesoporous channels of the support. The Ni-MAl catalysts also had significantly lower amounts of carbon deposited compared to the catalyst prepared using the co-precipitation method.

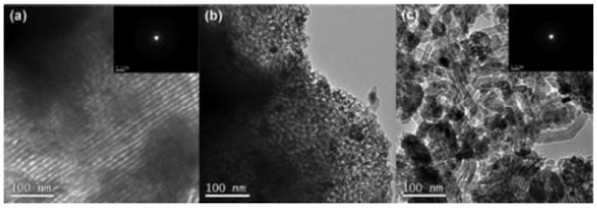

Fig. 9 TEM images of the 50 h endurance-tested M-5Ni5Ca90Al catalyst.[64]

Sokolov *et al*. prepared a series of supported Ni catalysts using various supports and tested them in DRM at 400 °C. Ni/La_2O_3-ZrO_2 showed near to equilibrium yields of CO and H_2 and the highest stability. Further, Ni containing nanostructured, mesoporous, and macroporous La_2O_3-ZrO_2 were studied. Among these materials only mesoporous materials exhibited practically no change in activity over 180 h on-stream, whereas the others deactivated. The formation of graphene like carbon layers on the catalysts and of NiO shell over Ni particles were found to be responsible for deactivation, while sintering of Ni did not play a major role. The enhanced stability of Ni on the mesoporous La_2O_3-ZrO_2 was attributed to the enhanced interaction of the Ni particles with the support arising from the pore confinement effect.[59]

Rivas *et al*. synthesized a series of Ni-based perovskite-type oxides $LaNiO_3$, $La_{0.8}Ca_{0.2}NiO_3$ and $La_{0.8}Ca_{0.2}Ni_{0.6}Co_{0.4}O_3$, as catalyst precursors in a highly ordered mesoporous SBA-15 silica host. All synthesized oxides showed a perovskite-type structure. Incorporation of the oxides into the mesoporous silica exhibited enhanced metal–support interaction increasing the Ni reduction temperature. A decrease in CH_4 and CO_2 conversion was observed when a second cation in A- and/or B site was added to the bulk perovskite. Alternatively, increases in conversions and selectivity at lower temperatures were observed in the case of mesoporous catalysts. H_2/CO molar ratio was found to be closer to one with no significant reduction in CH_4 conversion at 700 °C for 24h.[60] Wang *et al*., supported $LaNiO_3$ perovskite catalysts on mesoporous carriers ($LaNiO_3$/SBA-15, $LaNiO_3$/MCM-41 and $LaNiO_3/SiO_2$) with different pore structures. These have been synthesized via filling the pores of mesoporous silica with citrate complex precursors of nickel and lanthanum, with further treatments.[61] Catalytic performances were determined for DRM. XRD, N_2 physisorption and TEM analysis confirmed the formation of $LaNiO_3$ perovskite inside the pore channels of mesoporous supports. $LaNiO_3$/MCM-41 exhibited the highest initial catalytic activity, owing to the higher Ni dispersion, while $LaNiO_3$/SBA-15 was superior to $LaNiO_3$/MCM-41 in the long-term stability, which could be due to the stable silica matrix restricting the agglomeration of nickel species. The hexagonal mesopores of $LaNiO_3$/SBA-15 were still kept intact after reaction, while the mesoporous structure in $LaNiO_3$/MCM-41 collapsed during the reaction, which resulted in some metal particles aggregation. In comparison, the carbon deposition was responsible for the significant decrease in catalytic activity of a $LaNiO_3/SiO_2$ sample, evidenced by TGA and TPH results.

Very recently, Bao *et al*. synthesized bimodal pore NiCeMgAl catalysts via the refluxed co-precipitation method.[62] Methane dry reforming was systematically studied by optimizing the NiO loading, calcination temperature, reduction temperature and gas hourly space velocity (GHSV). The Ni15CeMgAl sample with 15 wt% NiO loading was found to be active enough at 750 °C with a high CH_4 conversion of 96.5%. The proper reduction temperature for the NiCeMgAl catalyst is either 550–650 °C or 850 °C with higher calcination temperature favoring the formation of $NiAl_2O_4$ and $MgAl_2O_4$. The Ni active sites derived from the $NiAl_2O_4$ spinel structure had longer stability than those from the free NiO. Compared with non-bimodal pore NiCeMgAl catalyst, bimodal pore NiCeMgAl catalyst has a longer stability in the feed gas without dilution. The large pores in the bimodal pore Ni15CeMgAl catalyst were assumed to contribute to the quick molecule transfer during dry reforming of methane (DRM) when the GHSV was less than 96,000 h^{-1}. Dacquin *et al*. used an in situ autocombustion route for synthesizing nanoscale NiO (3 nm) containing lanthanum-doped mesoporous silica composites.[63] Lanthanum is observed to cover the surface of the silica pore wall which might have had significant effect in reducing NiO sintering. Control over the size and size distribution of metallic nanoparticles clearly improved catalytic activity in DRM with enhanced stability which can be attributed to the presence of LaOx species. These materials were found to be stable at 700 °C for 48 h, with approximately 80 % conversions for both CH_4 and CO_2.

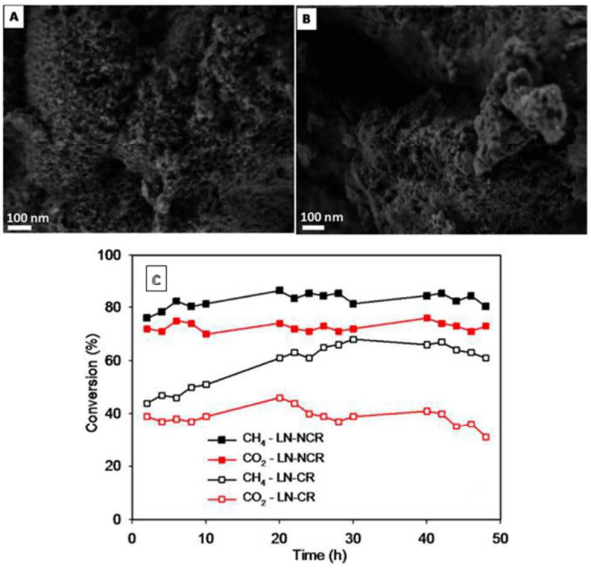

Fig. 10 (A) and (B) show high-resolution SEM images of the nanocast $LaNiO_3$ perovskite. (C) CH_4 and CO_2 conversions as a function of time on stream at 700 °C over Ni/La_2O_3 catalysts derived from nanocast (LN-NCR) and bulk $LaNiO_3$ (LN-CR) (GHSV = 2.1 × 10^5 h^{-1}).[65]

Xu *et al*. synthesized ordered mesoporous NiO–CaO–Al_2O_3 composite oxides with varying amounts of Ca by the EISA strategy.[64] These mesoporous materials exhibited higher activity as well as stability for DRM with retention of the mesotructure (Fig. 9). The authors suggested that the high specific surface area and large and uniform pore sizes inherent to these materials contributed to their superior performance. In addition, the confinement effect of the mesoporous matrixes stabilized the Ni active sites during the reaction conditions. Introduction of smaller amounts of Ca was found to increase the performance of these materials however with higher Ca amounts resulting in the reduction of activity. Nair *et al*. synthesized nanostructured Ni/La_2O_3 catalysts from nanocast mesoporous $LaNiO_3$ perovskites.[65] Ordered mesoporous SBA-15 silica was used as a hard template. These

materials were found to be efficient and stable catalysts for DRM. Nanocast perovskite with high specific surface area (150 m^2g^{-1}) was found to be transformed into Ni/La_2O_3 on performing reduction treatment at 700 °C. Approximately 90 % conversion was observed for both reactants over these novel mesoporous catalysts. Particularly, no coke formation was observed for 48 h, which reflects the enhanced stability of the catalyst obtained from the nanocast $LaNiO_3$ compared to the $LaNiO_3$ perovskite prepared by the citrate method (Fig.10). The improved performance of the nanostructured catalyst is attributed to the accessibility of the active sites resulting from the high specific surface area and the confinement effect leading to the stabilization of Ni nanoparticles.

Conclusions and Perspective

The design and preparation of coke resistant Ni catalysts remains the bottle neck for further development of CO_2 reforming of methane. The size, structure and nature of the catalyst have significant effects on its efficiency. If one can limit the Ni particle size below several nanometers under the reforming reaction conditions, the coke formation can be significantly controlled. However this remains a major challenge. A catalyst with good coke resistance is a must for the successful commercialization of DRM. One strategy that received considerable attention so far on this regard is to entrap Ni particles in well defined structure and here we briefly outlined the advancements achieved till now. It may be hypothesized that when metal (Ni) nanoparticles are supported on a basic oxide surface, the process by which coke deposition is present involves the reaction of CH_x species formed on the metal with surface carbonate species formed by reaction of CO_2 with surface basic sites. This oxidation process would prevent self-conversion of CH_x to larger carbonaceous species. In these conditions the proximity at atomic level of the metal particle and the basic site is a requirement owing to the lake of mobility of both reactive species. This would explain why coke resistant catalysts can be obtained by reduction of such mixed oxides as $LaNiO_3$ perovskites, which would preserve the initial proximity of Ni and La ions. Mesostructured mixed oxide materials are promising on this regard since they allow a better control of the metal migration upon reduction. Initial studies performed over such materials provided promising results. The development of novel solid solutions containing Ni with well-defined structures or entrapped in mesostructured materials will be interesting. For this, the development of novel catalyst preparation methods such as nanocasting is especially important.

Acknowledgements

The authors gratefully acknowledge the financial support of the Natural Sciences and Engineering Council of Canada.

Notes and references

1 T. Sakakura, J. Choi, and H. Yasuda, *Chem. Rev*., 2007, **107**, 2365; M. Aresta, A. Dibenedetto, and A. Angelini, *Chem. Rev*., 2014, **114**, 1709.

2 W. Wang, S. Wang, X. Ma and J. Gong, *Chem. Soc. Rev*., 2011, **40**, 3703; C. Costentin, M. Robert and J. Saveant, *Chem. Soc. Rev*., 2013, **42**, 2423; I. Shown, H. Hsu, Y. Chang, C. Lin, P. K. Roy, A. Ganguly, C. Wang, J. Chang, C. Wu, L. Chen and K. Chen, *Nano Lett*., 2014, **14**, 6097.

3 D. Baudouin, K. C. Szeto, P. Laurent, A. De Mallmann, B. Fenet, L. Veyre, U. Rodemerck, C. Copéret, and C. Thieuleux, *J. Am. Chem. Soc*., 2012, **134**, 20624; D. Pakhare and J. Spivey, *Chem. Soc. Rev*., 2014, **43**, 7813; D. Li, Y. Nakagawa and K. Tomishige, *Appl. Catal. A: Gen.,* 2011, **408**, 1.

4 A. Wörner and R. Tamme, *Catal. Today*, 1998, **46**, 165; S. Wang, G. J. Miller and G. Q. Lu, *Energy Fuels*, 1996, **10**, 896.

5 M. S. Fan, A. Z. Abdullah, and S. Bhatia, *ChemSusChem*, 2011, **4**, 1643; C. Liu, J. Ye, J. Jiang, and Y. Pan, *ChemCatChem*, 2011, **3**, 529.

6 A. Topalidis, D. E. Petrakis, A. Ladavos, L. Loukatzikou and P. J. Pomonis, *Catal. Today*, 2007, **127**, 238; A. D. Ballarini, S. R. de Miguel, E. L. Jablonski, O. A. Scelza and A. A. Castro, *Catal. Today*, 2005, **107–108**, 481.

7 M. C. J. Bradford and M. A. Vannice, *Catal. Rev. Sci. Eng*., 1999, **41**, 1; J. A. C. Dias and J. M. Assaf, *Catal. Today*, 2003, **85**, 59; T. Osaki and T. Mori, *J. Catal*., 2001, **204**, 89; S. Tang, L. Ji, J. Lin, H. C. Zeng, K. L. Tan and K. Li, *J. Catal*., 2000, **194**, 424; A. Djaidja, S. Libs, A. Kiennemann and A. Barama, *Catal. Today*, 2006, **113**, 194.

8 I. Rivaz, J. Alvarez, E. Pietri, M. J. Perez-Zurita and M. R. Goldwasser, *Catal. Today*, 2010, **149**, 388; G. Valderrama, M. R. Goldwasser, C. U. de Navarro, J. M. Tatibouet, J. Barrault, C. Batiot-Dupeyrat and F. Martinez, *Catal. Today*, 2005, **107**, 785.

9 Y. Wan and D. Zhao, *Chem. Rev*., 2007, **107**, 2821.

10 U. Chellam, Z. P. Zu and H. C. Zeng, *Chem. Mater*., 2000, **12**, 650; K. Pupovac and R. Palkovits, *ChemSusChem*, 2013, **6**, 2103; V. M. Gonzalez-delaCruz, R. Pereniguez, F. Ternero, J. P. Holgado and A. Caballero, *J. Phys. Chem. C*, 2012, **116**, 2919.

11 J. Guo, H. Lou, H. Zhao, D. Chai and X. Zheng, *Appl. Catal. A: General*, 2004, **73**, 75.

12 J. Guo, H. Lou, H. Zhao, D. Chai and X. Zheng, *React. Kinet. Catal. Lett*., 2005, **84**, 93.

13 N. Sahli, C. Petit, A. C. Roger, A. Kiennemann, S. Libs and M. M. Bettahar, *Catal. Today*, 2006, **113**, 187.

14 S. Corthals, J. V. Nederkassel, J. Geboers, H. D. Winne, J. V. Noyen, B. Moens, B. Sels and P. Jacobs, *Catal. Today,* 2008, **138**, 28.

15 L. Guczi, G. Stefler, O. Geszti, I. Sajo, Z. Paszti, A. Tompos and Z. Schay, *Appl. Catal. A: Gen.,* 2010, **375**, 236.

16 F. F. de Sousa, H. S. A. de Sousa, A. C. Oliveira, M. C. C. Junior, A. P. Ayala, E. B. Barros, B. C. Viana, J. M. Filho and A. C. Oliveira, *Int. J. Hydrogen Energy,* 2012, **37,** 3201.

17 R. Benrabaa, H. Boukhlouf, A. Lofberg, A. Rubbens, R. Vannier, E. Bordes-Richard and A. Barama, *J. Nat. Gas Chem*., 2012, **21**, 595; R. Benrabaa, A. Lofberg, A. Rubbens, E. Bordes-Richard, R. Vannier, and A. Barama, *Catal. Today*, 2013, **203**, 188.

18 R. Benrabaa, A. Lofberg, J. Caballero, E. Bordes-Richard, A. Rubbens, R. Vannier, H. Boukhlouf and A. Barama, *Catal. Commun*., 2015, **58**, 127.

19 L. Li, D. H. Anjum, H. Zhu, Y. Saih, P. V. Laveille, L. D'Souza and J. Basset *ChemCatChem,* 2015, **7**, 427.

20 S. A. Theofanidis, V. V. Galvita, H. Poelman and G. B. Marin, *ACS Catal*., 2015, **5**, 3028.

21 Y. Kathiraser, W. Thitsartharn, K. Sutthimporn and S. Kawi, *J. Phys. Chem. C*, 2013, **117**, 8120.

22 C. Batiot-Dupeyrat, G. Valderrama, A. Meneses, F. Martinez, J. Barrault and J. M. Tatibouet, *Appl. Catal. A: Gen.,* 2003, **248**, 143; M. R. Goldwasser, M. E. Rivas, E. Pietri, M. J. Pérez-Zurita, M. L. Cubeiro, L. Gingembre, L. Leclercq, and G. Leclercq, *Appl. Catal. A: Gen.,* 2003, **255**, 45.
23 M. R. Goldwasser, M. E. Rivas, E. Pietri, M. J. Perez-Zurita, M. L. Cubeiro, A. Grivobal-Constant and G. Leclercq, *J. Mol. Catal. A: Chemical,* 2005, **228**, 325.
24 C. Batiot-Dupeyrat, G. A. S. Gallego, F. Mondragon, J. Barrault and J. Tatibouet, *Catal. Today,* 2005, **107–108**, 474.
25 S. M. de Lima and J. M. Assaf, *Catal. Lett*., 2006, **108**, 63.
26 G. Valderrama, A. Kiennemann and M. R. Goldwasser, *Catal. Today,* 2008, **133**, 142.
27 M. E. Rivas, J. L. G. Fierro, M. R. Goldwasser, E. Pietri, M. J. Perez-Zurita, A. Griboval-Constant and G. Leclercq, *Appl. Catal. A: Gen.,* 2008, **344**, 10.
28 T. Johansson, D. Pakhare, D. Haynes, V. Abdelsayed, D. Shekhawat and J. Spivey, *Chem. Pap*., 2014, **68**, 1240.
29 G.S. Gallego, C. Batiot-Dupeyrat, J. Barrault, and F. Mondragon, *Ind. Eng. Chem. Res.,* 2008, **47**, 9272.
30 G. S. Gallego, C. Batiot-Dupeyrat, J. Barrault, E. Florez and F. Mondragon, *Appl. Catal. A: Gen.,* 2008, **334**, 251.
31 G. S. Gallego, J. G. Marin, C. Batiot-Dupeyrat, J. Barrault and F. Mondragon, *Appl. Catal. A: Gen.,* 2009, **369**, 97.
32 J. Gallego, C. Batiot-Dupeyrat, J. Barrault, and F. Mondragon, *Energy Fuels,* 2009, **23**, 4883.
33 R. Pereniguez, V. M. Gonzalez-DelaCruz, J. P. Holgado and A. Caballero, *Appl. Catal. B: Environ.,* 2010, **93**, 346.
34 R. Pereniguez, V. M. Gonzalez-delaCruz, A. Caballero and J. P. Holgado, *Appl. Catal. B: Environ.,* 2012, **123**, 324.
35 S. Pavlova, L. Kapokova, R. Bunina, G. Alikina, N. Sazonova, T. Krieger, A. Ishchenko, V. Rogov, R. Gulyaev, V. Sadykov and C. Mirodatos, *Catal. Sci. Technol*., 2012, **2**, 2099.
36 A. G. Bhavani, W. Y. Kim, and J. S. Lee, *ACS Catal*., 2013, **3**, 1537.
37 T. Odedairo, W. Zhou, J. Chen and Z. Zhu, *RSC Adv*., 2014, **4**, 21306.
38 Y. J. Su, K. L. Pan and M. B. Chang, *Int. J. Hydrogen Energy*, 2014, **39**, 4917.
39 L. De Rogatis, M. Cargnello, V. Gombac and B. Lorenzut, *ChemSusChem*, 2010, **3**, 24.
40 S. Zhang, J. Wang, H. Liu and X. Wang, *Catal. Commun*., 2008, **9**, 995; D. Liu, X. Y. Quek, W. N. E. Cheo, R. Lau, A. Borgna and Y. Yang, *J. Catal*., 2009, **266**, 380; D. Liu, R. Lau, A. Borgna and Y. Yang, *Appl. Catal. A: Gen.,* 2009, **358**, 110; D. Liu, X. Y. Quek, H. H. Adeline, G. Zeng, Y. Li and Y. Yang, *Catal. Today,* 2009, **148**, 243.
41 S. Wang and G. Q. (Max) Lu, *Energy Fuels,* 1998, **12**, 248-256; Wang and G. Q. (Max) Lu, *Appl. Catal. B: Environ.,* 1998, **16**, 269.
42 O. González, J. Lujano, E. Pietri and M. R. Goldwasser, *Catal. Today,* 2005, **107-108**, 436.
43 S. Damyanova, B. Pawelec, K. Arishtirova, J. L. G. Fierro, C. Sener and T. Dogu, *Appl. Catal. B: Environ.,* 2009, **92**, 250.
44 H. Arbag, S. Yasyerli, N. Yasyerli, G. Dogu, *Int. J. Hydrogen Energy,* 2010, **35**, 2296.
45 S. Yasyerli, S. Filizgok, H. Arbag, N. Yasyerli and G. Dogu, *Int. J. Hydrogen Energy,* 2011, **36**, 4863.
46 N. Wang, W. Chu, T. Zhang, X. S. Zhao, *Int. J. Hydrogen Energy,* 2012, **37**, 19.
47 S. Zhang, S. Muratsugu, N. Ishiguro, and M. Tada, *ACS Catal*., 2013, **3**, 1855.
48 M. Kaydouh, N. El Hassan, A. Davidson, S. Casale, H. El Zakhem, P. Massiani, *C. R. Chimie,* 2015, **18**, 293.
49 T. Xie, X. Zhao, J. Zhang, L. Shi and D. Zhang, *Int. J. Hydrogen Energy,* 2015, **40**, 9685.
50 Z. Liu, J. Zhou, K. Cao, W. Yang, H. Gao, Y. Wang and H. Li, *Appl. Catal. B: Environ.,* 2012, **125**, 324.
51 T. Xie, L. Shi , J. Zhang and D. Zhang, *Chem. Commun*., 2014, **50**, 7250.
52 Y. H. Guo, C. Xia and B. S. Liu, *Chem. Eng. J.* 2014, **237**, 421.
53 X. Du, D. Zhang, R. Gao, L. Huang, L. Shi and J. Zhang, *Chem. Commun*., 2013, **49**, 6770.
54 N. Sun, X. Wen, F. Wang, W. Wei and Y. Sun, *Energy Environ. Sci*., 2010, **3**, 366.
55 A. Peters, F. Nouroozi, D. Richter, M. Lutecki and R. Glaser, *ChemCatChem,* 2011, **3**, 598.
56 L. Xu, H. Songa and L. Chou, *Catal. Sci. Technol*., 2011, **1**, 1032.
57 W. Shen, H. Momoi, K. Komatsubara, T. Saito, A. Yoshida, S. Naito, *Catal. Today,* 2011, **171**, 150.
58 J. Newnham, K. Mantri, M. H. Amin, J. Tardio and S. K. Bhargava, *Int. J. Hydrogen Energy,* 2012, **37**, 454.
59 S. Sokolov, E. V. Kondratenko, M. Pohl, A. Barkschat, and U. Rodemerck, *Appl. Catal. B: Environ.,* 2012, **113–114**, 19.
60 I. Rivas, J. Alvarez, E. Pietri, J. Pérez-Zurita and M. R. Goldwasser, *Catal. Today,* 2010, **149**, 388.
61 N. Wang, X. Yu, Y. Wang, W. Chu and M. Liu, *Catal. Today,* 2013, **212**, 98.
62 Z. Bao, Y. Lu, J. Han, Y. Li and F. Yu, *Appl. Catal. A: Gen.,* 2015, **491**, 116.
63 J. Dacquin, D. Sellam, C. Dupeyrat, A. Tougerti, D. Duprez, and S. Royer, *Chemsuschem,* 2014, **7**, 631.
64 L. Xu, H. Song, and L. Chou, *ACS Catal*., 2012, **2**, 1331.
65 M. M. Nair, S. Kaliaguine, and F. Kleitz, *ACS Catal*., 2014, **4**, 3837

Graphical abstract

Structured Catalysts for Dry Reforming of Methane

Mahesh Muraleedharan Nair[a] and Serge Kaliaguine*[b]

[a] Department of Chemistry, Université Laval, Quebec city, G1V 0A6, Canada.

[b] Department of Chemical Engineering, Université Laval, Quebec city, G1V 0A6, Canada.

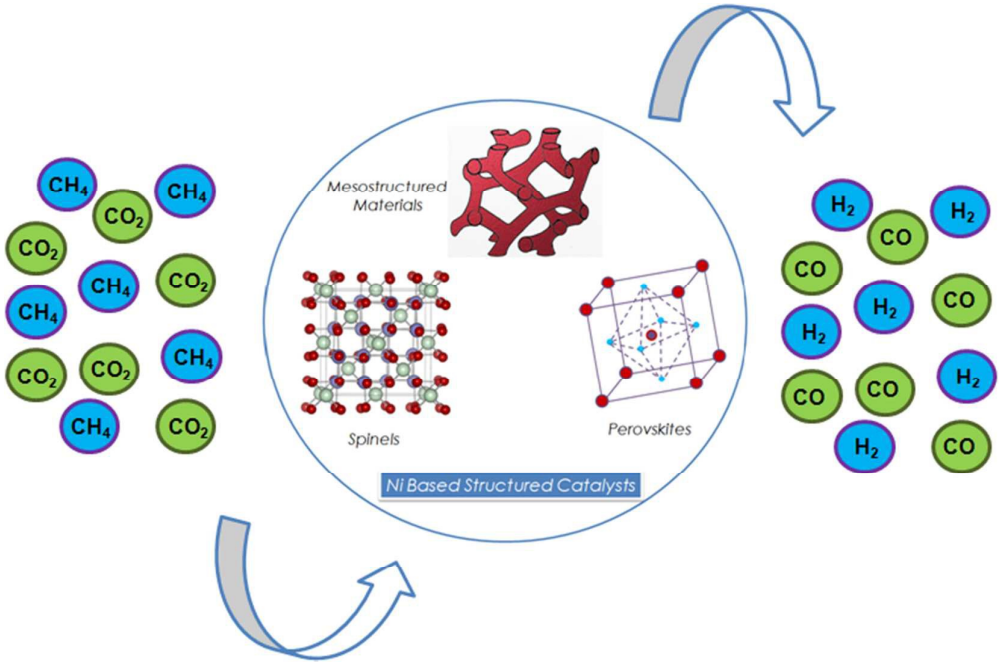

This review highlights the progress in designing oxide catalysts with well defined structures for dry reforming of methane